JOURNAL OF EXPERIMENTAL AND THEORETICAL PHYSICS, 2024, Vol. 165, No. 4, pp. 578–587

ELECTRONIC PROPERTIES OF SOLID

STRONG HALL EFFECT NONLINEARITY IN MACROSCOPICALLY MODULATED TWO-DIMENSIONAL SYSTEM

© 2024 A. V. Shupletsov[a,*], M. S. Nunuparov[b], K. E. Prikhodko[c,d], A. Yu. Kuntsevich[a,e]

[a] P.N. Lebedev Physical Institute of the RAS, 119991, Moscow, Russia

[b] Qmodule lab, 125493, Moscow, Russia

[c] National Research Center Kurchatov Institute, 123182, Moscow, Russia

[d] National Research Nuclear University MEPhI, 115409, Moscow, Russia

[e] National Research University Higher School of Economics, 101000, Moscow, Russia

Abstract. We study experimentally the low-temperature conductive properties of double-gate two dimensional array of islands in metal-oxide-semiconductor structure. The system appears to be a highly tunable two-dimensional metamaterial with diffusive transport and macroscopic modulation. In particular, we reveal several effects in magnetic field and gate voltages dependencies of the Hall coefficient, and Shubnikov-de Haas oscillations. In moderate magnetic fields 1T, the Hall effect carrier density demonstrates seemingly counterintuitive nonmonotonic behavior as function of gate voltage. This behavior, however, can be qualitatively described by mean-field approach for effective media. In small magnetic fields the strongest unexpected temperature- and gate-dependent Hall effect nonlinearity emerges, that can not be described by mean-field effective media theory. We argue that this effect can be related to weak-localization phenomena and current redistribution in inhomogeneous media. In the quantized magnetic field an unusual splitting of Shubnikov-de Haas resistivity minimum is observed. Our observation should stimulate studies of tunable modulated two-dimensional systems.

DOI: 10.31857/S004445102404e114

1. INTRODUCTION

Laterally modulated two-dimensional metamaterials are interesting both for novel physics and applications. Since 1990-s extensive experimental studies of conductive properties of two-dimensional (2D) systems with artificial voids have been performed, covering such aspects as ballistic transport [1–3], symmetry breaking [4], localization-delocalization transition [5–9], mesoscopic effects [10–12]. Besides arrays of voids in the 2D gas, it is possible to form periodic 2D structure from two types of areas with different properties, for example superconducting islands surrounded by 2D system, [13], or surface of 3D topological insulator with slight modulation of disorder [14]. Technology development and emergence of 2D materials made the modulated systems more sophisticated that led to the Moire modulated lateral superlattices, where perfect modulation of properties forms naturally [15–17] at the nano-level.

The modulation periodicity is believed to matter only if the superlattice period is smaller than the scattering lengthscales. Only few transport experiments are performed for the systems, where scattering lengths are less than the modulation period [6, 18].

In our paper we examine the low-temperature conductive properties, and particularly Hall effect, in the disordered and yet not insulating 2D system with square lattice of macroscopic round islands modulation. We

* E-mail: husderbec@mail.ru

demonstrate that low-temperature magnetotransport in such system is quite puzzling and may exhibit new dramatic effects.

For uniform system Hall effect should be independent of the sample geometry within the classic transport theory. It means that voids inside the 2D system should preserve the Hall voltage. Experimentally Hall effect in 2D systems with voids was studied in Refs. [18–20] and, surprisingly, the deviations from the classical behavior were detected. The field dependence originated either from quantum effects or additional length scales emergence.

Filling the voids with 2D gas leads to the transport properties change. In two-component modulated system Hall effect value is expected to lie between the Hall effect of the components. This understanding is in accordance with theoretical predictions [21–25]. Sharp magnetic field dependence of the Hall coefficient is not anticipated.

In order to test the role of macroscopic modulation we take the most well-known 2D system: Si-MOS structure with 2D gas in the inversion channel. Two subsystems – islands array and the rest 2D gas – are independently controlled by spatially separated gate electrodes. This system is somewhat similar to granular materials, studied broadly in the past [26]. The islands array differs from granular systems by: (i) complete two-dimensionality and tunability of both islands and surrounding gas; (ii) periodicity, i.e. absence of randomness in the islands positions; (iii) absence of sharp boundaries between surrounding gas and islands due to electrostatic nature of gating.

In fixed magnetic field ∼1T Hall effect of the islands array could be well understood within effective media theory for two-component system. In smaller magnetic field we uncover a strong non-linearity of the Hall effect, i.e. field-dependent Hall coefficient. This non-linearity decreases with temperature rise and may even changes from upturn to downturn for different gate voltages. We connect this behavior with weak localization (WL) effect and qualitatively describe it through simple considerations about current redistribution.

2. SAMPLES

We used Si-MOSFET structures with lithographically defined islands array (IA). Voltages applied to two electrically decoupled gate electrodes independently control the electron density (i) in the islands (V_i) and (ii) in the surrounding 2D gas (S2DG) (V_g). Panels **a**, **b** in Figure 1 show optical images of the sample. The IA has a Hall-bar shape with lateral dimensions 0.4mm x 0.4mm, islands diameter 2.5 μm and lateral period d 5 μm. Therefore transport between the islands is diffusive ($l \ll d$, where mean free path $l \sim 50$ nm in the highest mobility samples) and possible coherent effects are negligible ($l_\phi < d$ where coherence length $l_\phi < 500$ nm in studied temperature range).

The STEM images (see example in Figures 1**c** and 1**d**) were obtained using FEI Titan 80-300 microscope at the electron energy of 200 keV. The cross-section thin lamella for TEM studies was cut out from the surface region using FEI Helios NanoLab 650 focused ion beam. The cut was made along the side of the square sample through the diameters of the islands (shown by dashed line in panel **b** of Figure 1).

Panels 1**c** and 1**d** demonstrate the sample profile in the direction perpendicular to the 2D gas plane. The bottom gray layer is the crystalline (001) Si substrate; the dark color corresponds to SiO_2. The investigated 2D gas is formed at the interface between the Si substrate and the oxide layer. The gates are made of polycrystalline heavily doped Si (gray areas above SiO_2). The layer indicated as V_g is S2DG gate and has a sieve shape, as shown in yellow in Fig.1**e**. This electrode is covered by another layer of SiO_2. On the TEM images S2DG gate is a trapezoidal area surrounded by oxide layers. The gate of the islands V_i is placed above, so that it is continuous through the whole system. 2D gas outside the islands is shielded by S2DG gate from voltage V_i. Panel 1**d** shows a zoom in of the edge of the island. Gate electrodes are separated by oxide so that there is an area (shown as 2 in Fig. 1**e**) between the islands and the S2DG where oxide layer is thicker. The electron density in such areas, hereafter called *shells*, is expected to be lower.

Hall bars without modulation were defined on the same chip and allowed to get the pristine 2D gas properties.

3. RESULTS

Magnetoresistance measurements were performed in the temperature range 0.3-8 K using Cryogenics 21T/0.3K and CFMS 16T/1.8K systems. All measurements were carried out in the frequency range 13-18 Hz using standard 4-terminal lock-in amplifier technique at 100 nA transport current to avoid overheating. To compensate for contact asymmetry, magnetic field was swept from positive to negative values. Resistance per square ρ (Hall resistance R_{xy}) data were then symmetrized (antisymmetrized). All measurements were performed in the regime where $\rho < h/e^2$.

The experiments were carried out on several samples with peak Hall mobility ranging from 500 to 3000 cm^2/Vs. The mobility had impact only on the magnitude of the effects. We demonstrate the representative data from the high (IA1) and low (IA2) mobility samples.

3.1. Hall density

The effective Hall density ($n_{eff}^{exp} \equiv [eR_{xy}(B = 1\text{T})]^{-1}$) and carrier mobility ($\mu_{eff} \equiv (n_{eff}^{exp} e\rho)^{-1}$) were calculated from ρ and R_{xy} at $\pm$1T. This field is the compromise value, where quantum effects don't show up: WL is suppressed and Shubnikov-de Haas oscillations (SdHO) don't emerge yet.

We analyzed the n_{eff}^{exp} dependencies on V_g and V_i. In the uniform Si inversion layers electron density is roughly proportional to $(V_{gate} - V_{th})$. Here V_{th} is a threshold voltage ($\sim$1 V) that originates from the charge stored in the oxide and the work function difference between the gate and 2D system [27]. $n_{eff}^{exp}(V_g)$ dependencies (shown in Figure 2 for various V_i values) are in contrast with this expectation.

For V_g high enough (shown by **(a)** and **(b)** in Figure 2) S2DG is very conductive due to high electron density. Islands are surrounded by the shells with lower electron density, i.e. by poorly conductive areas. As a result, the transport current flows predominantly through the S2DG, i.e. $n_{eff}^{exp}(V_g)$ is mainly determined by the S2DG.

Nevertheless, the current partially flows through the islands that causes the $n_{eff}^{exp}(V_i)$ dependence. For rather high V_i (**(a)** in Figure 2) the concentration in the islands is higher than in the S2DG. With the increase of V_i the concentration and conductivity in the islands grow that leads to the increase of current fraction through them. As a result, n_{eff}^{exp} rises with V_i.

One of the conspicuous features of the $n_{eff}^{exp}(V_g)$ dependence is the curves intersection for low V_i. It can be explained taking into account the gate voltage dependence of the mobility. This dependence for the pristine 2DEG is shown in the inset to Figure 3. The mobility in Si-MOSFETs grows dramatically with V_{gate} close to the threshold value [27]. It leads to the stronger increase of the current fraction flowing through low-density regions comparing with their density increase. It results in n_{eff}^{exp} value drop with V_i. In the limit of fully depleted islands n_{eff}^{exp} is defined by the S2DG concentration. As V_i increases, the islands become weakly conductive, and the current begins to flow through them. Therefore n_{eff}^{exp} decreases.

A similar reasoning can be applied to the region of small V_g and large V_i values (**(d)** in Figure 2). The islands are much more conductive than S2DG, therefore current flows through them minimizing the path through the S2DG. S2DG density increases with V_g and S2DG mobility rises even stronger. The increase of the low-density S2DG contribution to the Hall effect overwhelms the increase of S2DG density. It leads to the n_{eff}^{exp} decrease with V_g. The contribution of depleted S2DG rises with V_i decrease that leads to the disappearance of upturn (**(c)** in Figure 2).

An upturn for high V_i and low V_g shifts to plain for lower V_i. The region (c) differs from sample to sample. For some samples it even transforms to downturn.

The effective density demonstrates similar gate dependence for various mobility samples (see inset to Figure 2).

The observed dependencies were compared with the mean field analytical expressions [24]. The model system consists of the regular array of equivalent circular regions with radius R and period a embedded into a conductive matrix. Mean field approach works the better the less occupation factor p comparing to the percolation threshold p_c [28,29]. For isotropic 2D system $p_c = 0.5$ therefore we suggest that the mean field theory for our system with $p = \frac{\pi R^2}{a^2} \approx 0.2$ is justified. The components of the effective conductivity tensor σ_{xx}^e and σ_{xy}^e are expressed through σ_{xx}^i, σ_{xy}^i of the islands (i=1) and S2DG (i=2). Correspondingly, effective concentration n_{eff}^{th} is equal to $\frac{B}{e\rho_{xy}^e} = B\frac{(\sigma_{xx}^e)^2+(\sigma_{xy}^e)^2}{e\sigma_{xy}^e}$. The conductivity tensors of the subsystems are substituted in Drude's

form into Eq.A7 of Ref. [24]: $\sigma^i_{xx} = \frac{n_i e \mu_i}{1+(\mu_i B)^2}$ and $\sigma^i_{xy} = \mu_i B \sigma^i_{xx}$ (i=1 corresponds to the islands and i=2 to the S2DG).

As a result, we obtain $n^{th}_{eff} = f(n_1, \mu_1, n_2, \mu_2, B)$. The dependencies $\mu(V_{gate})$ and $n(V_{gate})$ for pristine 2D gas (shown on the inset in Figure 3) are obtained from the homogeneous MOSFET on the same chip. $n(V)$ is approximated by a linear function, $\mu(V)$ - by a polynomial one. Thus, the effective concentration depends on three variables: $n^{th}_{eff}(V_g, V_i, B) = f(n(V_i), \mu(V_i), n(V_g), \mu(V_g), B)$, where V_g is the gate voltage for S2DG and V_i – for islands.

$n^{th}_{eff}(V_g)$ theoretical dependencies for B=1T for three different V_i values are shown in Figure 3. Mean field results reproduce well all features of the experimental $n^{exp}_{eff}(V_g)$ dependence from Figure 2: (i) linear behavior for high V_g, (ii) low-V_g transition from linear to upturn with V_i, and (iii) low-V_i intersect at moderate V_g.

3.2. Magnetotransport

We performed detailed magnetotransport measurements in different regimes of current flow: **b**, **c**, and **d** (here and further designations are taken from Figure 2) .

Figure 4(a) shows resistivity and Hall coefficient $R_H(B) \equiv R_{xy}(B)/B$ in the regime **d**, where transport is dominated by the islands. Hall coefficient acquires B-dependence. Though ρ is about 15 kOhms (i.e. $\sim e^2/h$), pronounced SdHO are observed due to the high mobility in the islands. Electron density obtained from SdHO ($n_{SdH} \approx 1.4 \times 10^{12}$ cm^{-2}) corresponds to the islands, and is higher than the Hall density ($n^{exp}_{eff} \lesssim 1 \times 10^{12}$ cm^{-2}) because the latter is affected by both S2DG and islands. Hall coefficient has a *maximum* at $B = 0$ and growing trend for high magnetic fields. Interestingly, both zero field feature and SdHO are more pronounced in Hall coefficient than in ρ_{xx}.

Figure 4(b) shows resistivity and R_H in the regime **b** with $V_i = 0$. V_g was adjusted to set n^{exp}_{eff} approximately equal to that from Figure 4(a). $\rho \approx$ 3kOhms is about 5 times less because S2DG is well-conductive and current bypasses the depleted regions. SdHO are observed with $n_{SdH} \approx 0.9 \times 10^{12}$ cm^{-2} comparable to $n^{exp}_{eff} \lesssim 1.2 \times 10^{12}$ cm^{-2}. Due to strong $n^{exp}_{eff}(B)$ dependence, the equality $n^{exp}_{eff} = n_{SdH}$ is reached in the field ∼3T, where SdHO occur. Hall coefficient has *minimum* at $B = 0$ and growing trend for higher magnetic field.

Finally, Figure 4(c) shows resistivity and R_H in low-density regime **c**. The gate voltages were adjusted to make ρ approximately equal to the value from Figure 4(a). The transport behavior is qualitatively similar to Figure 4(b) without SdHO. Hall coefficient has *minimum* at $B = 0$ grows with field.

The common tendency for all $R_H(B)$ data is the growth with field. In homogeneous system Hall coefficient is constant: $R_H = 1/ne$. In the studied system there are regions with different densities. For Si-MOSFETs electron mobility is density-dependent (see inset in Figure 3 or [27]). In magnetic field the longitudinal conductivity $\sigma_{xx} \propto (1 + (\mu B)^2)^{-1}$, i.e. the higher the mobility, the faster the decrease with B. Thus, the conductivity of low-density regions decreases slower with field than for high-density regions, thus the current fraction through low-density regions increases and the R_H rises.

In small magnetic field $R_H(B)$ dependence experiences an abrupt feature. The bare 2D gas in Si-MOSFETs has a small low-field Hall nonlinearity [30]. However, its *huge* amplitude in Figure 4(a-c) clearly identifies it with the sample nonuniformity. This enormously large non-linearity is one of the main observations of our paper.

Previously low-field transverse magnetoresistance quenching (even sign change) was observed in artificially inhomogeneous ballistic systems. Experiments in 1D wires by Roukes [19] were further theoretically explained [31] by electron trajectories scrambling near the contacts. In further experiments with ballistic antidot arrays [1] the Hall effect quenching was observed, although the qualitative pinball picture didn't account for it. In the later experiments [20] the quenching was confirmed by numerical simulations, but no physical mechanism was suggested.

Our system is essentially different, because the transport is diffusive and the inhomogeneities are tunable from low ("dots", $V_i > V_g$) to high ("antidots" $V_i < V_g$) potential. Low-field Hall coefficient either grows or falls with B depending on V_g and V_i. $R_H(B \to 0)$ quenching suppression with temperature (Figure 4(d) for IA2) indicates that this feature can be related to WL. This assumption is nontrivial. Firstly, it is a textbook knowledge that in homogeneous medium WL doesn't influence the Hall resistance [32,33]. Secondly, the nonlinearity scale is rather high (few 10%), larger than WL correction to resistivity in the bare 2D gas.

Due to current redistribution with magnetic field Hall effect nonlinearity might emerge that was shown in Ref. [24]. Indeed, due to WL the mobility becomes field-dependent with a minimum at $B = 0$. The WL relative effect on mobility depends on carrier density: for large n it is inversely proportional to $n\mu$ (see eq. 3 in Ref. [24]). Therefore this effect is stronger for lower densities. However, when n becomes low and the conductivity approaches the quantum one, the WL amplitude is suppressed [34, 35].

These considerations can qualitatively explain the observed dependencies in Figure 4. For example, Figure 4(a) corresponds to high concentration in the islands and partially depleted S2DG. The field dependence of the S2DG mobility due to WL is suppressed therefore relative increase of the mobility in the islands is higher. The current redistribution with field occurs in favor of the islands, i.e. Hall coefficient decreases. In Figure 4(b-c) the islands aren't conductive but surrounded by low density shells. The shells conductivity grows faster with field than that for S2DG therefore the current redistributes in favor of them resulting in Hall coefficient rise. In Figure 4(d) the islands and S2DG conductivities are big and different, therefore Hall coefficient increases with field as explained above. Thus low-field Hall nonlinearity can be explained qualitatively but its huge amplitude and strong temperature dependence remain puzzling.

Another unusual high-field magnetotransport effect is SdHO minima splitting in ρ_{xx} (see dashed rectangles in Figure 4(a-b) and Figure 4(e)). As a rule, resistivity maxima are split in the high enough field when Zeeman energy exceeds the temperature and Landau level broadening. Indeed, in uniform 2D systems Hall resistance ρ_{xy} is higher than ρ_{xx} in SdH domain. Therefore the conductivity maxima $\sigma_{xx} = \rho_{xx}/(\rho_{xx}^2 + \rho_{xy}^2) \approx \rho_{xx}/\rho_{xy}^2$ at the half-integer filling factors (density of states maxima) correspond to the resistivity maxima. The mean-field approximation model with the conductivity tensors of subsystems with the SdHO included eq. (3.24) and (3.25) in Ref. [36]) can get a locally similar picture (Figure 4(f)) though SdHO phase mainly remains unchanged. It means that the minima splitting can't be explained by the change of the oscillations phase and Zeeman splitting. However, the observed feature can emerge due to the oscillations in low-density subsystem on the background of the main high-density (i.e. high-frequency) subsystem. It's noteworthy that ρ_{xx} minimum is split even when islands aren't conductive (Fig. 4(b)). It means that shells role is crucial for the description of this feature.

A complete theory explaining all observed features beyond the two-component mean field approach [24] must take into account the transport through the shells. Existing magnetoresistance mechanism beyond the mean field theory is the resistivity tensor components mixing [37] for $\mu B \gg 1$. In our case μB is not high enough.

Our results should facilitate the studies of magnetotransport in the modulated two-dimensional systems, and particularly in the systems where such modulation forms spontaneously [38].

4. CONCLUSIONS

To sum up, we experimentally examined transport properties of the macroscopically modulated and tunable 2D metamaterial based on Si-MOS technology, where both density and modulation depth are controlled separately. Nonlinear dependencies of the effective Hall density on gate voltages could be well explained qualitatively and quantitatively within the mean field theory. We also explore temperature dependent unexpectedly strong low-field Hall effect nonlinearity, that should be related to weak localization, and unusual splitting of Shubnikov-de Haas oscillations resistivity minima. Our data call for theoretical explanation and studies in less ubiquitous material systems.

The work is supported by MD-1571.2022.1.2 Presidential grant by the Ministry of Science and Higher Education of the Russian Federation.

REFERENCES

1. D. Weiss, M. L. Roukes, A. Menschig, et al., Phys. Rev. Lett. **66**, 2790 (1991).

2. D. Weiss, K. Richter, A. Menschig, et al., Phys. Rev. Lett. **70**, 4118 (1993).

3. D. A. Kozlov, Z. D. Kvon, A. E. Plotnikov, et al., JETP Lett. **89**, 80 (2009).

4. K. Tsukagoshi, S. Wakayama, K. Oto, et al., Phys. Rev. B **52**, 8344 (1995).

5. A. Dorn, Th. Ihn, K. Ensslin, et al., Phys. Rev. B **70**, 205306 (2004).

6. G. M. Minkov, A. A. Sherstobitov, A. V. Germanenko and O. E. Rut, Phys. Rev. B **78**, 195319 (2008).

7. N. E. Staley, N. Ray, M. A. Kastner, et al., Phys. Rev. B **90**, 195443 (2014).

8. S. Goswami, M. A. Aamir, C. Siegert, et al., Phys. Rev. B **85**, 075427 (2012).

9. V. A. Tkachenko, O. A. Tkachenko, G. M. Minkov and A. A. Sherstobitov, JETP Lett. **104**, 473 (2016).

10. F. Nihey, S. W. Hwang and K. Nakamura, Phys. Rev. B **51**, 4649 (1995).

11. Y. Iye, M. Ueki, A. Endo and S. Katsumoto, Jour. Phys. Soc. Jap. **73**, 3370 (2004).

12. R. Yagi, M. Shimomura, F. Tahara, et al., Jour. Phys. Soc. Jap. **81**, 063707 (2012).

13. Zh. Han, A. Allain, H. Arjmandi-Tash, et al., Nat. Phys. **10**, 380 (2014).

14. H. Maier, J. Ziegler, R. Fischer, et al., Nat. Comm. **8**, 2023 (2017).

15. C. R. Dean, L. Wang, P. Maher, et al., Nature **497**, 598 (2013).

16. Y. Cao, V. Fatemi, A. Demir, et al., Nature **556**, 80 (2018).

17. Y. Cao, V. Fatemi, Sh. Fang, et al., Nature **556**, 43 (2018).

18. A. Yu. Kuntsevich, A. V. Shupletsov and M. S. Nunuparov, Phys. Rev. B **93**, 205407 (2016).

19. M. L. Roukes, A. Scherer, S. J. Allen, et al., Phys. Rev. Lett. **59**, 3011 (1987).

20. S. de Haan, A. Lorke, R. Hennig, et al., Phys. Rev. B **60**, 8845 (1999).

21. R. H. Bube, App. Phys. Lett. **13**, 136 (1968).

22. J. Heleskivi and T. Salo, Jour. Appl. Phys. **43**, 740 (1972).

23. C. J. Adkins, Jour. Phys. C: Sol. St. Phys. **12**, 3389 (1979).

24. A. Yu. Kuntsevich, A. V. Shupletsov and A. L. Rakhmanov, Phys. Rev. B **102**, 155426 (2020).

25. B. Sanvee, J. Schluck, M. Cerchez, et al., Phys. Rev. B **108**, 035301 (2023).

26. B. Abeles, P. Sheng, M. D. Coutts and Y. Arie, Adv. in Phys. **24**, 407 (1975).

27. Ts. Ando, A. B. Fowler and F. Stern, Rev. Mod. Phys. **54**, 437 (1982).

28. L. D. Landau, L. P. Pitaevskii and E. M. Lifshitz, *Electrodynamics of Continuous Media*, Butterworth-Heinemann, Oxford, UK, 1984.

29. A. P. Vinogradov, *Electrodynamics of Composite Materials*, URSS, Moscow, 2001.

30. A. Yu. Kuntsevich, L. A. Morgun and V. M. Pudalov, Phys. Rev. B **87**, 205406 (2013).

31. C. W. Beenakker and H. van Houten, Phys. Rev. Lett. **63**, 1857 (1989).

32. H. Fukuyama, Jour. Phys. Soc. Jap. **49**, 644 (1980).

33. B. L. Altshuler, D. Khmel'nitzkii, A. I. Larkin and P. A. Lee, Phys. Rev. B **22**, 5142 (1980).

34. M. Rahimi, S. Anissimova M. R. Sakr, et al., Phys. Rev. Lett. **91**, 116402 (2003).

35. G. M. Minkov, A. V. Germanenko and I. V. Gornyi, Phys. Rev. B **70**, 245423 (2004).

36. A. Isihara and L. Smrcka, Jour. Phys. C: Sol. St. Phys. **19**, 6777 (1986).

37. M. M. Parish and P. B. Littlewood, Nature **426**, 162 (2003).

38. V. M. Pudalov, JETP Lett. **116**, 456 (2022)

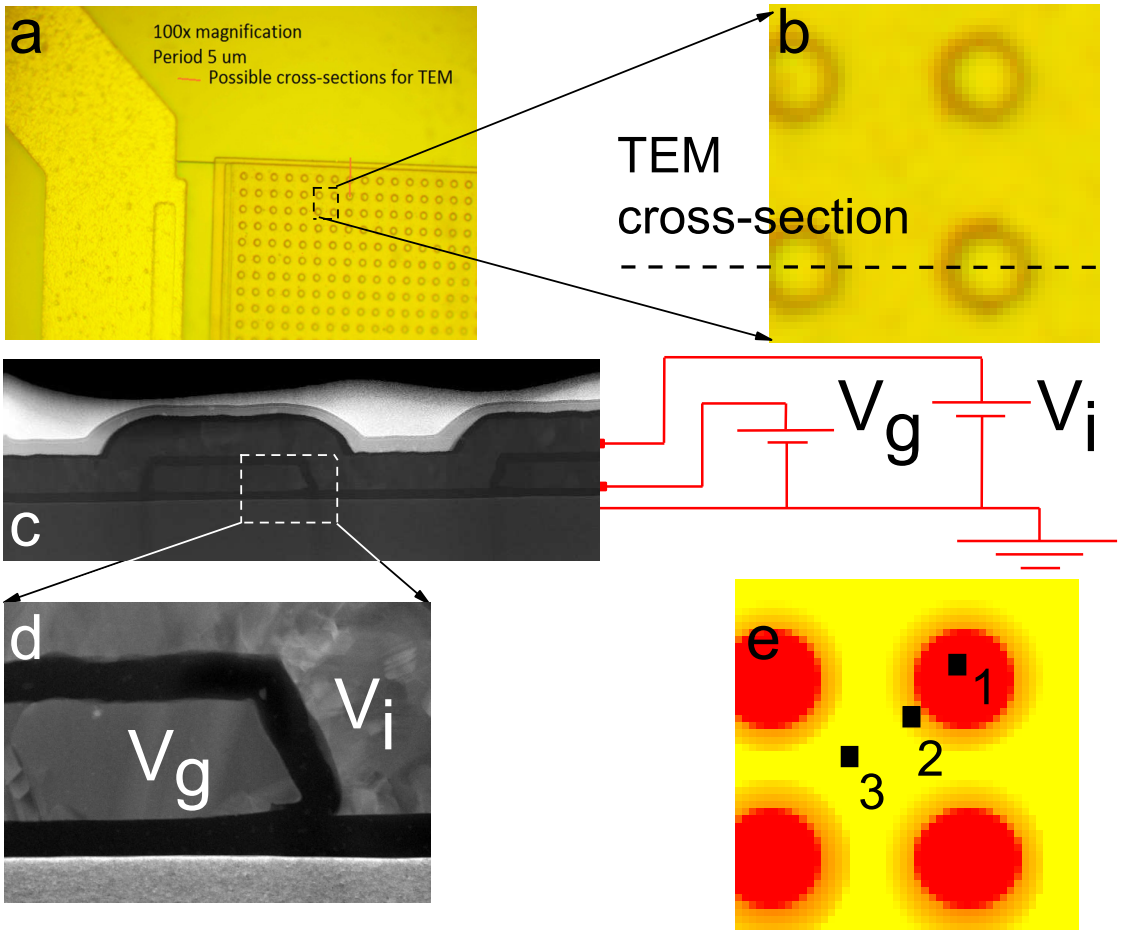

Fig. 1. (a) Optical microscope image of the IA corner (100x magnification), (b) zoom-in of (a) showing TEM slice direction, (c) STEM image with the gating scheme, (d) zoom-in of (c) showing the island (on the right) and S2DG (on the left) gates, (e) schematic map of the modulated system with color indication (red (1) for islands; orange (2) for shell; yellow (3) for S2DG).

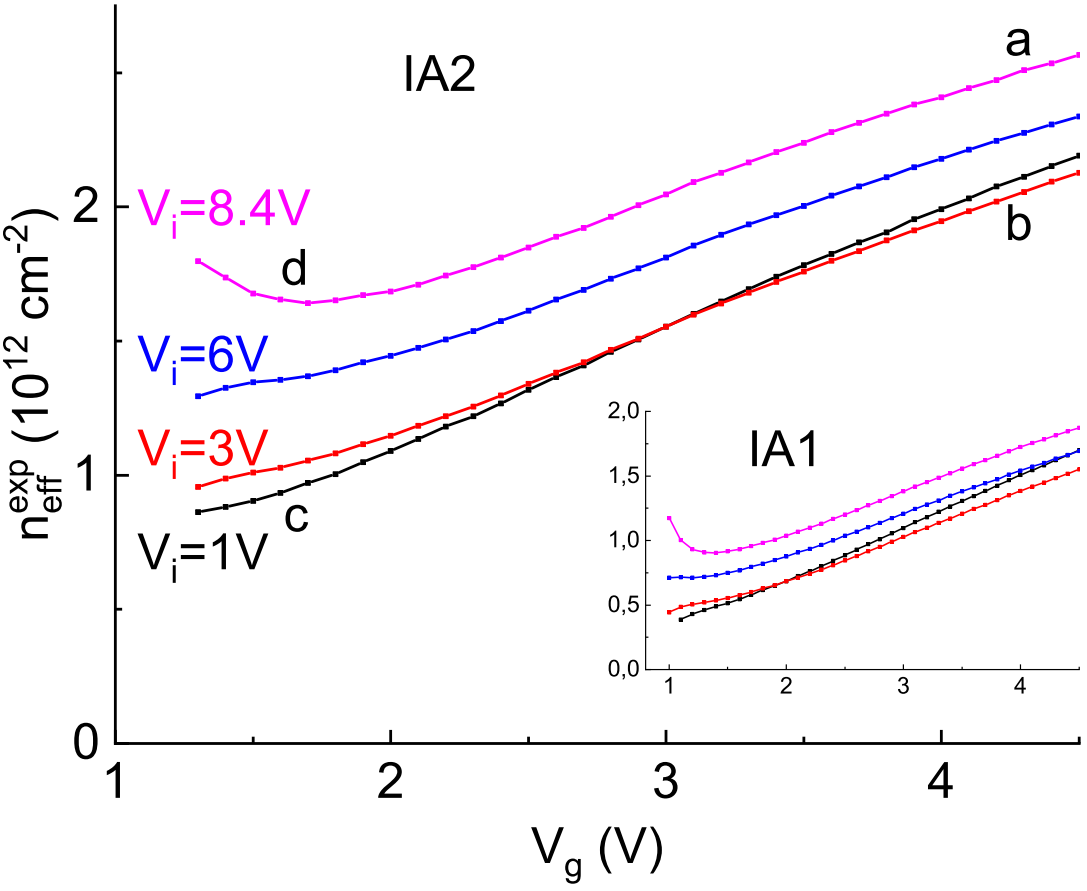

Fig. 2. The Hall density at T=1.8 K for IA2 vs S2DG gate voltage V_g for representative islands gate voltages V_i (indicated in the panel). The inset shows the similar data for IA1 for the same values of V_i.

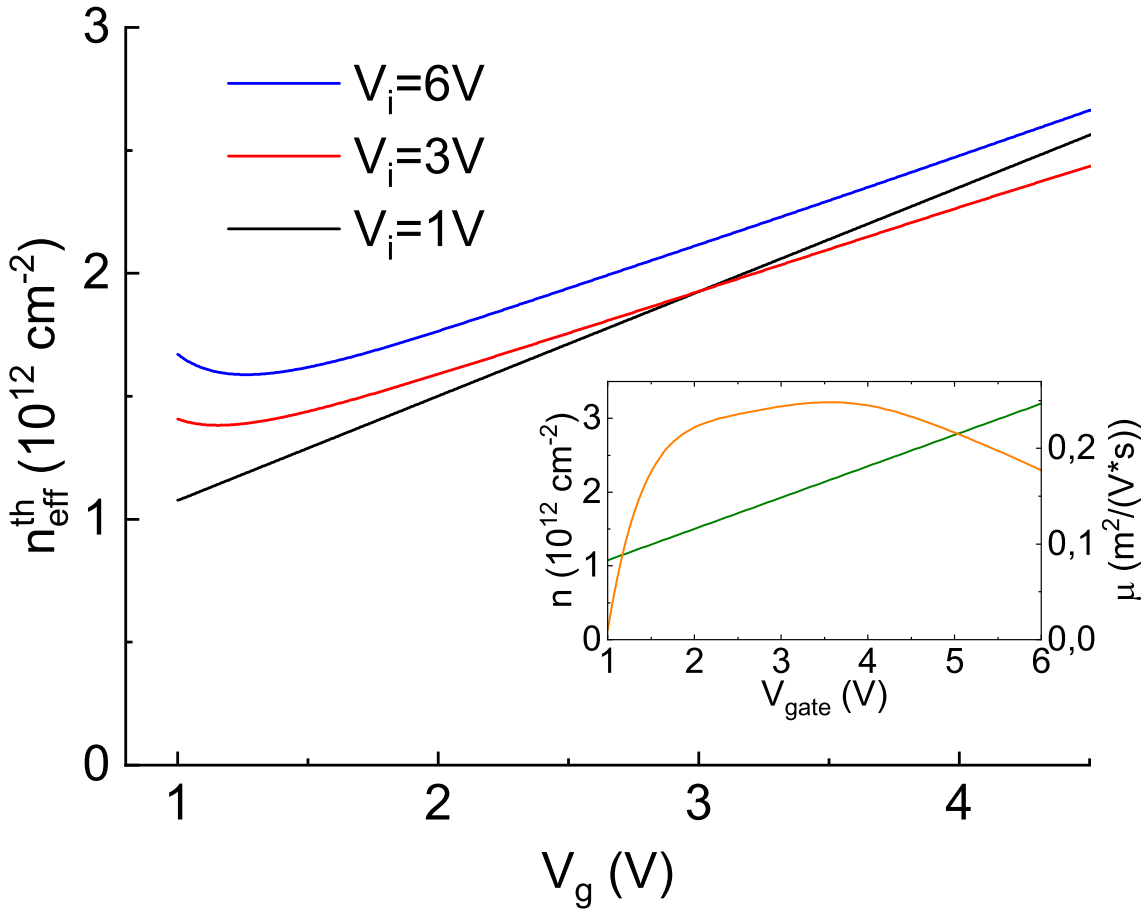

Fig. 3. Effective concentration n_{eff}^{th} dependence on the V_g obtained from the theory for V_i (1V, 3V and 6V), calculated for $B = 1$ T. The inset demonstrates the experimental gate dependence of the mobility (orange) and the concentration (green) of the pristine electron gas at T=1.8 K used in calculations.

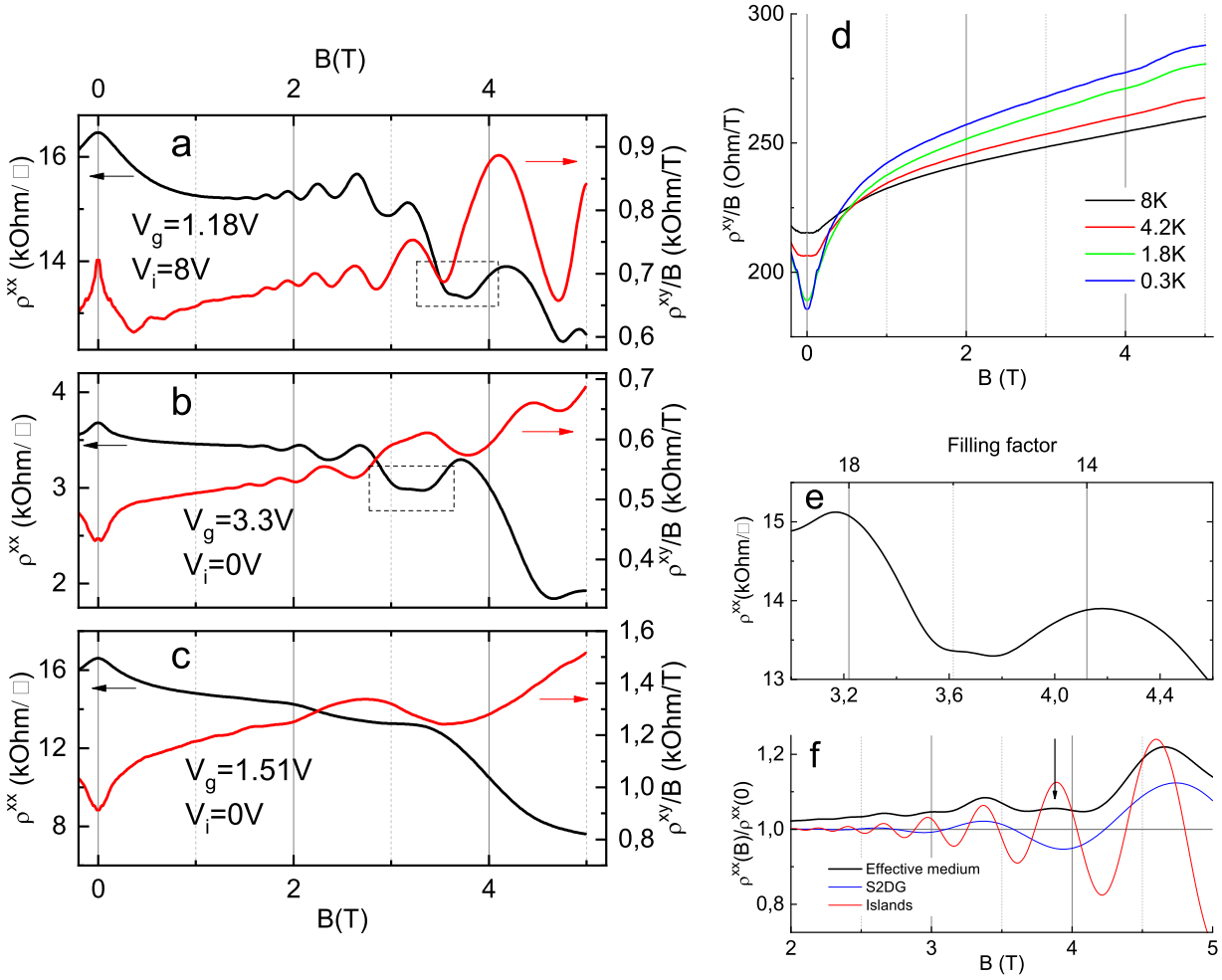

Fig. 4. (a-c) Resistivity (black) and Hall coefficient (red) of the IA1 at $T = 0.3$K: (a) current through the islands; (b-c) current through S2DG with effective density (b) and $B = 0$ resistivity (c) close to (a). (d) Hall coefficient of the IA2 ($V_g = 4$V and $V_i = 2.5$V) vs magnetic field for different temperatures. (e) Enlarged area from (a) shown by dashed rectangle that demonstrate the resistivity minimum splitting. (f) Theoretical magnetic field dependence of relative resistivity for the effective medium (black), islands (red) and S2DG (blue). The concentration and mobility in the islands are 1.22×10^{12} cm^{-2} and 0.4 m^2/(V·s), in the S2DG — 0.56×10^{12} cm^{-2} and 0.28 m^2/(V·s). The arrow indicates the area similar to panel (e).